Advances in Concrete Construction, *Vol. 7, No. 4 (2019) 249-262*
DOI: https://doi.org/10.12989/acc.2019.7.4.249

Shear strengthening of deficient concrete beams with marine grade aluminium alloy plates

Adi S. Abu-Obeidah[1], Jamal A. Abdalla[2] and Rami A. Hawileh[*2]

[1]Department of Civil Engineering, Rutgers, The State University of New Jersey, USA
[2]Department of Civil Engineering and Materials Science and Engineering Research Institute (MSERI), American University of Sharjah, UAE

(Received December 30, 2018, Revised April 12, 2019, Accepted April 19, 2019)

Abstract. In this study, high strength aluminum alloys (AA) plates are proposed as a new construction material for strengthening reinforced concrete (RC) beams. The purpose of this investigation is to evaluate AA plate's suitability as externally bonded reinforcing (EBR) materials for retrofitting shear deficient beams. A total of twenty RC beams designed to fail in shear were strengthened with different spacing and orientations. The specimens were loaded with four-points loading till failure. The considered outcome parameters included load carrying capacity, deflection, strain in plates, and failure modes. The results of all tested beams showed an increase up to 37% in the load carrying capacity and also an increase in deflection compared to the control un-strengthened beams. This demonstrated the potential of adopting AA plates as EBR material. Finally, the shear contribution from the AA plates was predicted using the models available in the ACI440-08, TR55 and FIB14 design code for fiber reinforced polymer (FRP) plates. The predicted results were compared to experimental testing data with the ratio of the experimentally measured ultimate load to predicted load, range on the average, between 93% and 97%.

Keywords: aluminum alloy; shear capacity; externally bonded plates; FRP; reinforced concrete

1. Introduction

Shear failure in reinforced concrete (RC) beams is a catastrophic type of failure that usually happens suddenly without any warnings and for that reason it is highly recommended to ensure flexure strength governs in concrete beams rather than shear (Jumaat *et al*. 2011). Shear Deficiencies occur for several reasons, including insufficient shear reinforcement, reduction in steel rebar area because of corrosion, service load increase, or construction defects (Mesbah and Benzaid 2017, Zhichao and Hsu 2005, Adhikary and Mutsuyoshi 2005, Hawileh *et al*. 2018, Khalifa and Nanni 2000, Triantafillou 1998, Al-Sulaimani *et al.* 1994, Täljsten and Elfgren 2000, Chajes *et al*. 1995). Externally bonded reinforcement (EBR), if applied properly, provides an excellent solution in upgrading the shear capacity of structural elements. The most common techniques available for shear and flexural strengthening of RC structures are bonding with steel plates, FRP laminates or their hybrid combinations (Chakrabortty and Khennane 2014, Sumathi and Vignesh 2017, Hawileh *et al*. 2014). These techniques have proven to be effective in many studies and applications when bonded externally as studied by several investigators (Hosseinpour and Abbasnia 2014, Hosseinpour and Abdelnaby 2015, Razavi *et al*. 2015, Esfandiari and Esfandiari 2016, Abdel-Kareem 2014, Metwally 2014, Wang and Su 2013, Ali *et al*. 2014, Abdul Samad *et al*. 2017, Wu *et al*. 2012, Akroush *et al*. 2017, Aykac *et al*. 2013, Foster *et al*. 2017, Baghi and Barros 2016, Hawileh *et al*. 2014, Hawileh *et al*. 2015). On the other hand, few shortcomings for the same techniques have been reported such as the low corrosion resistance and the heavy weight of the steel plates (Kissell and Ferry 1995, Abu-Obeidah *et al*. 2015) and the lower thermal resistance and brittle behavior of the FRP laminates (Hameed *et al*. 2018, Wu *et al*. 2012, Azam and Soudki 2014). It is important to investigate new techniques in strengthening RC structural components that could extend the service life of the structure. Aluminum alloy plates have high potential in serving as externally bonded strengthened materials for both shear and flexure that could overcome the reported shortcomings of FRP and steel if applied properly.

Aluminum as a metal is considered to have the required mechanical properties to function as a major structural member in any system (Xing and Osman 2016, Szumigała and Polus 2015). Some of the unique structural properties of AA plates are being isotropic, ductile, high thermal resistance, high corrosion resistance, and its high strength to weight ratio. In addition, Researchers discussed some of the AA types that have great potential to be used as externally bonded reinforcement for concrete structures such as aluminum alloy series 5000, 6000, and 7000 (Abdalla *et al*. 2016, Dursun and Soutis 2014). These alloys are usually utilized in ship buildings, pressure vessels, aerospace industries and some structural components for their high tensile strength. Moreover, aluminum galvanic corrosion is not an issue that could affect the durability of the strengthening system or the composite, since this corrosion

∗Corresponding author, Professor
E-mail: rhaweeleh@aus.edu

http://www.techno-press.org/?journal=acc&subpage=7
ISSN: 2287-5301 (Print), 2287-531X (Online)

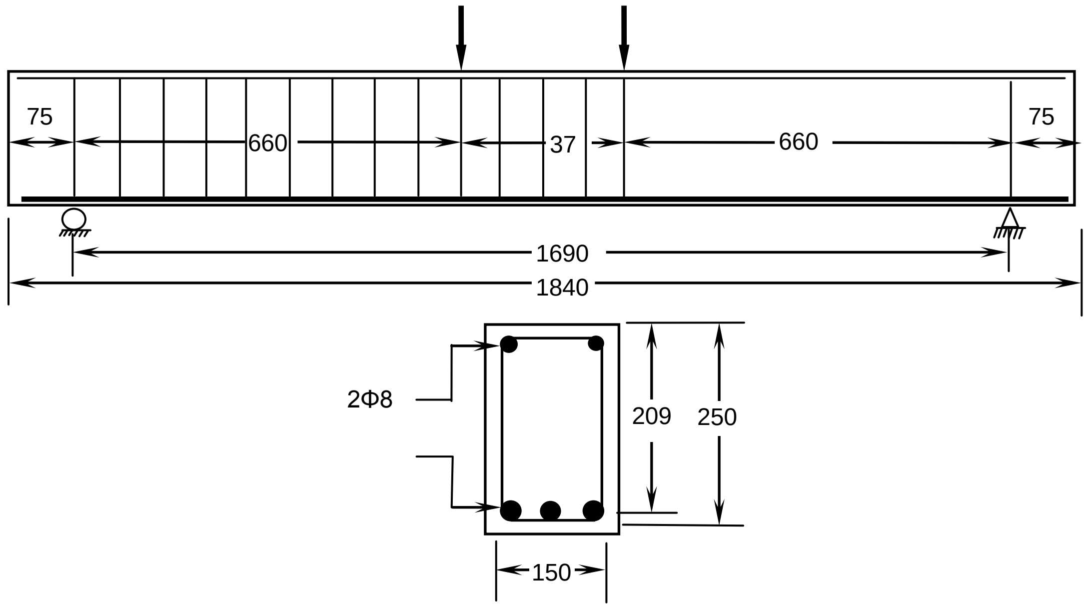

Fig. 1 Beam detailing and cross-section (all dimensions are in mm)

type only happens when soluble calcium chloride is present in the concrete along with the aluminum is in direct contact as discussed intensively in many studies (Jana and Tepke 2010, Editorial Report 1965, McGeary 1966, Linberg 1960). For this study, a layer of epoxy/resin is applied between the concrete and the AA plates, which eliminates the galvanic corrosion risk.

The literature review has revealed that strengthening with AA plates is a promising technique for RC members that should be further investigated. For instance, Rasheed *et al*. (2017) strengthened ten flexural deficient concrete beams with 2 and 3 mm AA plates and the results presented showed that the beams' flexural capacity was improved up to 40% compared to the control un-strengthened specimen. In addition to that, the current authors, in previous papers studied the behavior of AA shear strengthened beams experimentally and analytically (Abdalla *et al*. 2011, Abu-Obeidah *et al*. 2012). Abdalla *et al*. (2016) in a previous pilot study tested five shear deficient RC beams that were externally strengthened in shear with AA plates. They observed that the capacity of the strengthened specimens has increased between 24-89% compared to the un-strengthened beam. The shear capacity of the strengthened beams was also predicted using the ACI440, FIB14, TR55, and SMCFT design guidelines with the later one giving the most accurate predictions. For the same specimens, 3D nonlinear finite element (FE) models were also developed to capture and predict the response of such strengthened beams and close agreement between the predicted and measured results was found at most of the stages of loading (Abu-Obeidah 2012).

In addition to the applications in flexural and shear strengthening, the AA plate's bond-slip properties to concrete was recently investigated (Abdalla *et al*. 2017, Mirghani *et al*. 2017). The authors tested the bond stress-slip behavior of AA plates bonded to concrete surface with different AA surface roughness. This phenomenon directly correlates to the plate effectiveness when utilized for strengthening. Twelve specimens with six different surface roughness were instrumented and tested under single shear and the results showed that the bond stress, loading capacity, and failure modes vary with the variation of the surface roughness or the bonded length or both. The shear capacity and maximum bond stress increased by 143.6 and 342.6%, respectively, for randomly grinded surface compared with those of normal surface for a bonded length of 75% of the plate. The work on this topic is still limited and for that, this study aims to further investigate the effectiveness and feasibility of using externally bonded AA plates in strengthening eighteen shear deficient RC beams. In particular the objectives are to: (1) investigate the effect of externally bonded AA reinforcement ratio, spacing and orientation on the load-carrying capacity, failure mode, and deflection and (2) predict the AA shear contribution by the different formulas developed for FRP in several codes and compare it with the obtained experimental results.

2. Test program

The testing program focused on investigating the shear performance of simply supported RC beams externally strengthened with AA plates. A total of twenty shear-deficient RC beams were tested under four point loading. Two un-strengthened beams served as control beams and eighteen beams were strengthened with AA plates. All beams were strengthened with 3 mm thick AA plates on one side of the beam's specimen that was not reinforced in shear by stirrups. The experimental variables included the total plates length bonded on each side, spacing, and orientations of the plates.

2.1 Strengthened speicmen details

A total of twenty rectangular reinforced concrete beams were fabricated to be strengthened with stirrups in one side

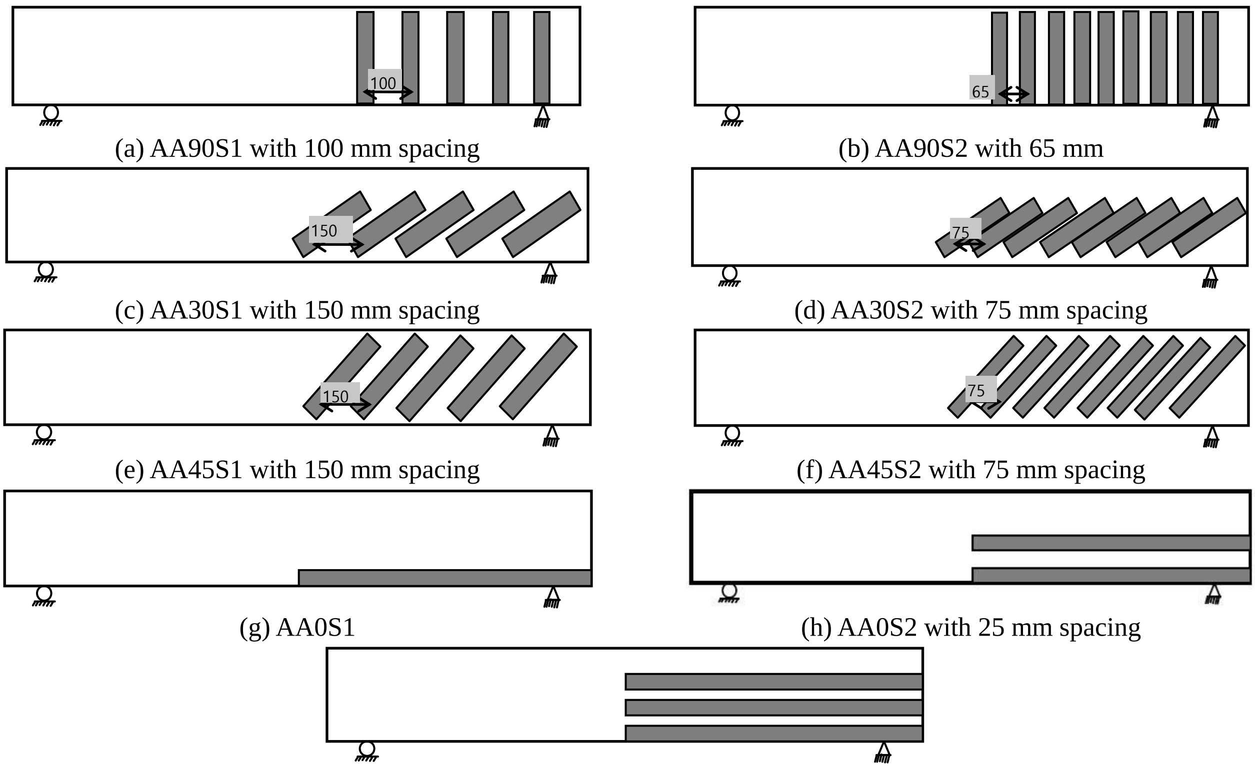

(a) AA90S1 with 100 mm spacing
(b) AA90S2 with 65 mm
(c) AA30S1 with 150 mm spacing
(d) AA30S2 with 75 mm spacing
(e) AA45S1 with 150 mm spacing
(f) AA45S2 with 75 mm spacing
(g) AA0S1
(h) AA0S2 with 25 mm spacing
(i) AA0S3 with 10 mm spacing

Fig. 2 Test matrix showing shear reinforcement scheme and spacing of AA plates

(#8 mm @ 50 mm) and shear deficient on the other side (no stirrups), which restricts the AA plate's application to be on one side only as shown in Fig. 1. In flexure, the beams were reinforced with 3#19 mm bars in the tension zone located at a depth of 209 mm from the beam's top surface. Two beams were tested as reference specimens (no AA plates) and eighteen were externally strengthened with AA plates as shown in Fig. 2. All AA plates utilized have slenderness (width/thickness) of 16.67. Also, all beams are 1840 mm long by 150 mm wide by 250 mm deep with a span length of 1690 mm. The shear span zone, which is 660 mm, begins from the loading point and ends at the supporting point as shown in Fig. 1.

Fig. 2 shows the detailed strengthening system adopted in this study. The beam designation for each strengthened beam is AAZST, where AA for Aluminum Alloy, Z for the orientation angle measured from the longitudinal axis of the beam, S for spacing with the digit 1, 2 or 3 to indicate different spacing, and N for the spacing configuration number of AA plates used to strengthen the beam. As presented in Fig. 2, the specimens are designated as follow:

a) AA**90**S1 and AA**90**S2 designate beams strengthened with **90**^{o} plates spaced at 100 and 65 mm center-to-center (cc), respectively.

b) AA**45**S1 and AA**45**S2 designate beams strengthened with **45**^{o} plates spaced at 150 and 75 mm, respectively.

c) AA**30**S1 and AA**30**S2 designate beams strengthened with **30**^{o} plates spaced at 150 and 75 mm, respectively.

d) AA**0**S1, AA**0**S2 and AA**0**S3 designate beams strengthened with **180**^{o} AA plates that are spaced at 25 mm for AA**0**S2 and 10 mm for AA**0**S3.

With the Exception of AA**0**S specimens, all specimens were externally strengthened with 50×200×3 mm thick AA plates with different orientations and horizontal spacing as presented in Fig. 2. AA**0**S1, AA**0**S2 and AA**0**S3 were strengthened with 50×1000×3 mm at different vertical spacing and quantities. For more consistent results, two specimens were tested from each category of beams and the average of the test results was adopted. The strengthening procedure of the tested beams included surface preparation by randomly grinding the shear face of the concrete beam and the AA plates to create a rough surface and ensure maximum bond stress. Then, epoxy resins are applied on both surfaces and the plates are bonded to the concrete surfaces.

2.2 Material properties

2.2.1 Concrete and steel reinforcement

The average compressive stress of the concrete used to cast all the specimens was 37.2 MPa. Concrete cylinders are made on site with the beams and were tested on the same testing day for each beam specimen. For the steel reinforcement, three 300 mm bars were tested at a rate of 10 mm/min with a gage length of 200 mm. The average yield strength and modulus of elasticity was 590.4 MPa and 199.9 GPa, respectively.

2.2.2 Aluminum Alloy (AA) plate

Marine grade Aluminum Alloy (AA) 5083-H111 is the type of AA plate utilized in this study. The chemical composition of the AA alloy is summarized in Table 1. This

Table 1 Chemical composition, physical and mechanical properties of 5083-H111 aluminum alloy (Aalco Metals Limited 2017)

Chemical Properties		Physical and Mechanical Properties	
Chemical element	% Present	Property	Value
Aluminum, Al	93.9%	Density	2.65 g/cm³
Chromium, Cr	0.05-0.25%	Melting Point	570 °C
Copper, Cu	0.10%	Thermal Expansion	25×10^{-6} /K
Iron, Fe	0.40%	Modulus of Elasticity	72 GPa
Magnesium, Mg	4.0-4.9%	Thermal Conductivity	121 W/m.K
Manganese, Mn	0.40-1.00%	Electrical Resistivity	0.058×10^{-6} Ω.m
Other (each)	0.0-0.05%	Density	2.65 g/cm³
Other (total)	0.0-0.15%	Proof Stress	125 Min MPa
Silicon, Si	0.0-0.40%	Tensile Strength	275-350 MPa
Titanium, Ti	0.05-0.25%	Elongation A50 mm	23 %
Zinc, Zn	0.108%	Shear Strength	175 MPa
-	-	Hardness Brinee	75 HB

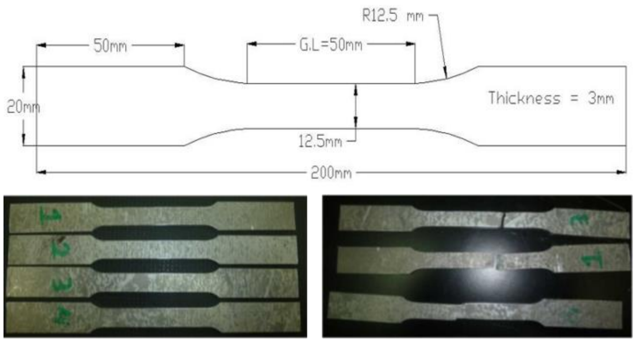

(a) Coupon specimen details

Fig. 3 Coupon tests of AA specimens

alloy is usually used in highly stressed welded assemblies, dump truck boxes, vehicle bodies, rail cars, shipbuilding, storage tanks, pressure, and cryogenic vessels (Aalco Metals Limited 2017). The tensile strength, yield strength and modulus of elasticity of AA plates are 288.6 MPa, 148.8 MPa, and 70.3 GPa respectively.

To verify the AA mechanical properties, three identical specimens have been shaped, cut and prepared according to the ASTM-B557M specification to perform coupon testing as shown in Fig. 3. As presented, each coupon has a total length of 200 mm, width of 20 mm and gauge length of 50 mm. Fig. 3 (b) and (c) show the specimens before and after the tensile testing. It should be noted that all coupon specimens failed within the gage length, as expected and presented in Fig. 3(c).

The obtained stress-strain curves from the tensile test results are presented in Fig. 4 and Table 2. The average values for the yield strength, ultimate tensile stress and modulus of elasticity are 148 MPa, 305.25 MPa and 71 GPa, respectively. The percentage difference in the mechanical properties measured in the laboratory is within

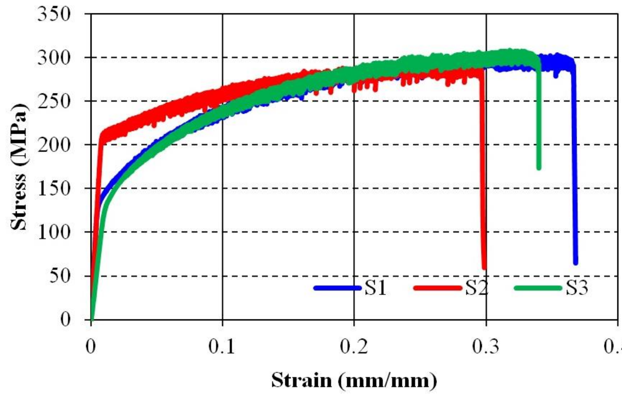

Fig. 4 Sample coupon results for AA5083-H111

Table 2 Aluminum properties

	f_y (MPa)	f_u (MPa)	Elongation (%)
S1	135	302.2	35.3
S2	214.03	293.74	29.2
S3	131	308.29	32.2
Average	160.01	301.41	32.23
Specifications	148	288.60	20.9
Percent Difference (%)	8.11	4.44	54.23

10% difference when compared to the manufacturer's certificate. On the other hand, the percentage difference in the elongation reached 54.23% which could indicates that the manufacturer's certificates are slightly conservative.

2.2.3 Epoxy adhesives

Sikadur-30LP was the epoxy utilized to bond the AA plates to the shear span of RC beam specimens. It is a Structural two-component adhesive, based on a combination of epoxy resins and especially designed for use at higher temperatures between +25℃ and +55℃. After properly mixing the 2-components properly, the epoxy should be applied within 30 to 60 minutes, which is the pot life. The minimum expected compressive, flexural, and shear strength of the epoxy adhesive at +25°C are 85, 25, and 17 MPa, respectively as reported by the manufacturer.

2.3 Material properties

All the beams were tested under four point bending and loaded monotonically using a digitally controlled INSTRON 8806 Universal Testing Machine (UTM) that has a capacity of 2500 kN, at a rate of 10 kN/min until failure. In order to capture the AA plates strain during testing, strain gauges were installed on some of the plates that are expected to capture the highest stress according to their location with respect to the shear crack. There are some cases where the crack propagates around the plates instead of penetration through it which presented in low strain measurements as shown in Fig. 5. Two sizes of strain gauges, 5 and 10 mm were installed at the same plate orientation degree which is also presented in Fig. 5.

3. Results and discussion

Fig. 5 Strain gauges installed on AA plates

Table 3 Summary of test results

	P_u	$P_{u(avg)}$	% increase of P_u over CB	Deflections			Ductility Index	
				δy	δu	δf	$\delta f/\ \delta u$	$\delta f/\ \delta y$
CB1	119.40	118.40	-	5.11	5.11	5.11	1.00	1.00
CB2	117.40		-	3.83	6.51	7.01	1.08	1.83
AA90S1-1	139.53	129.47	18	5.74	5.74	5.75	1.00	1.00
AA90S1-2	119.40		1.0	5.46	5.46	6.78	1.24	1.24
AA90S2-1	126.48	137.06	7.0	6.96	6.96	6.96	1.00	1.00
AA90S2-2	147.63		25	6.16	7.82	9.09	1.16	1.48
AA30S1-1	143.48	140.06	21	5.90	7.70	7.80	1.01	1.32
AA30S1-2	136.63		15	4.70	8.20	9.70	1.18	2.06
AA30S2-1	126.48	124.78	7.0	4.80	4.80	5.40	1.13	1.13
AA30S2-2	123.08		6.0	4.19	5.00	5.52	1.01	1.32
AA45S1-1	129.45	146.12	9.0	6.10	6.10	6.80	1.11	1.11
AA45S1-2	162.79		37	6.29	8.23	9.57	1.16	1.52
AA45S2-1	145.17	151.50	23	5.67	7.96	10.02	1.26	1.77
AA45S2-2	157.83		33	6.69	6.69	7.20	1.08	1.08
AA0S1-1	132.19	130.04	12	4.82	7.47	8.04	1.08	1.67
AA0S1-2	127.89		8.0	6.65	6.65	6.85	1.03	1.03
AA0S2-1	140.47	148.74	19	5.96	5.96	6.54	1.10	1.10
AA0S2-2	157.00		33	7.71	7.71	8.26	1.07	1.07
AA0S3-1	160.74	159.51	36	5.48	7.76	8.43	1.09	1.54
AA0S3-2	158.27		34	6.76	6.76	6.95	1.03	1.03

The results for each specimen in terms of the ultimate carrying capacity (P_u), deflections at the flexural reinforcement yield point (δ_y), at the ultimate capacity point (δ_u) and at the failure point of the specimens (δ_f) which correlates to 80% of the ultimate load are all provided and summarized in Table 3. In addition, two ductility indices for each specimen are calculated as an indication of the AA plate's effectiveness in improving the composite beam deflection. The ratio of the deflection at failure to the deflection at ultimate ($\delta_f/\ \delta_u$) in the first ductility index and the ratio of the deflection at failure to the deflection at yield (δ_f/δ_y) is the second one. Although the indices showed minor improvement in the ductility in most specimens, it is still an important outcome in evaluating the proposed material and technique. Generally, the AA plates significantly increased the ultimate load-carrying capacity

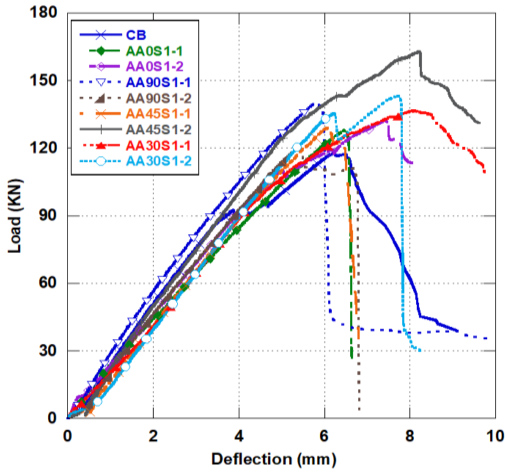

(a)

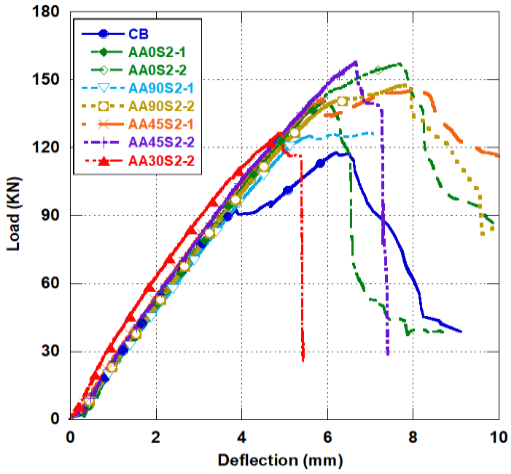

(b)

Fig. 6 Load-deflection response for (a) S1 and (b) S2 specimens

of the RC beams up to 37% over the control (un-strengthened) beam. The deflection at ultimate load in the strengthened specimens reached up to 8.23 mm, compared with a deflection of 5.81 mm in the control beam, representing a maximum increase of 41.6%. The structural behavior of the beams is discussed in terms of load deflection response and failure modes in the following subsections.

3.1 Load-deflection and strain response curves

As presented in Figs. 6-10, the resulted load-deflection and load-plate strain response curves of the strengthened beams are almost bilinear, indicating the brittle nature of most shear failures. Fig. 6 shows the effect of the strengthening material orientation (AA0, AA45, AA90, AA30) on the load-deflection response of beams strengthened with AA plates, compared with the control beam. Two control beams (CB1, CB2) were tested and failed in shear with a capacity of 117 kN and 119 kN, respectively.

As shown in Fig. 6, the beams that were strengthened with 0°, 90°, 30°, and 45° plates failed at ultimate maximum

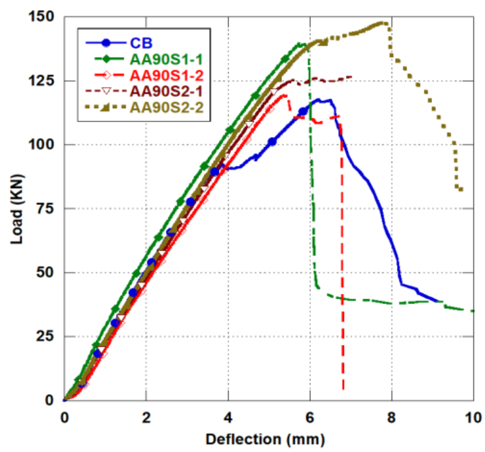

(a)

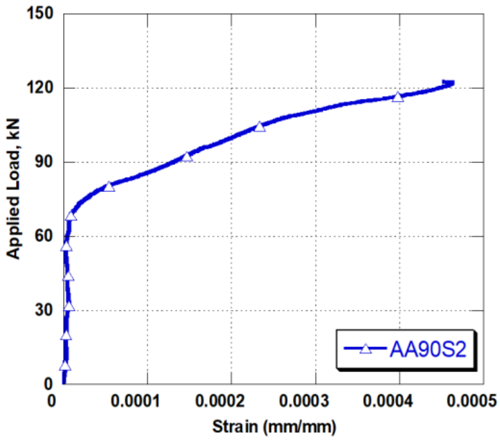

(b)

Fig. 7 Load deflection and strain results for AA90 beams (a) Load deflection response for AA90S1 and AA90S2 beams (b) A plate Strain results for AA90S2 specimen

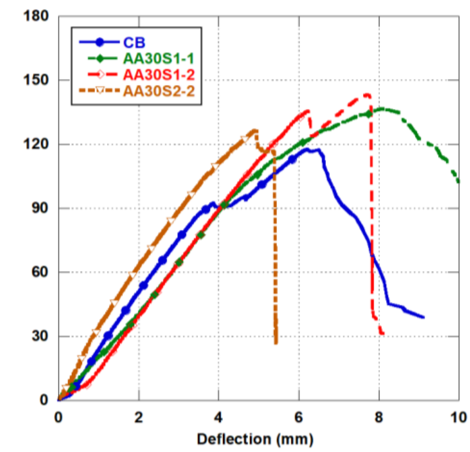

(a)

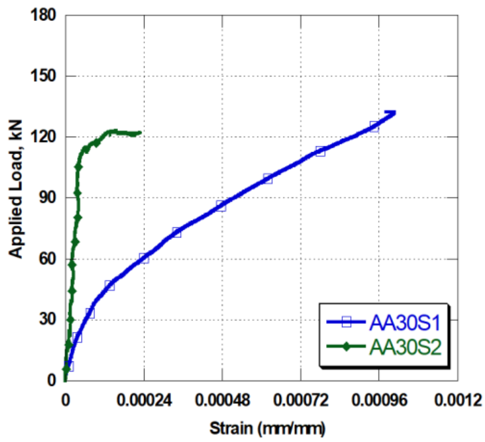

(b)

Fig. 8 Load deflection and strain results for AA30 beams (a) Load deflection response for AA30S1 and AA30S2 beams (b) AA plate Strain results for AA30S1 and AA30S2 specimen

loads of 132.2, 139.5, 143.5, and 162.8 kN, respectively for S1 specimens which correlates with an increase in the ultimate load by 12, 18, 21, and 37%. For S2 beams, the 0^o, 90^o, 30^o, and 45^o specimens failed at maximum ultimate loads of 157, 147.6, 126.7, and 157.8 kN, respectively for S2 specimens which correlates with a percentage increase by 33, 25, 7, and 33%. Based on these results, the beam strengthened with 45^o plates (AA45S1-2) experienced the highest improvements in load (37% increase) and deflection at ultimate compared to the control beam. For the same specimen (AA45S1-2), the deflection at ultimate load reached up to 8.23 mm, representing an increase of 41% compared with the CB average deflection (5.81 mm). For the other S1 and S2 specimens, the deflection increased up to 32.7%, 34.6% and 41.1% for AA0, AA90 and the AA30 specimens, respectively compared to the control beam average deflection. As observed, the increase in the plate's quantity did not correlate consistently with the specimens shear capacity increase and this will be explained further in the following sections.

Figs. 7-10 presents the load-deflection response of the strengthened beams with the same orientation angle at different spacing and quantities. As shown in Fig. 7, AA90S1 specimens achieved an increase in the capacity up to 18% compared to the control beam with no significant change in deflection. However, the shear capacity increased up to 25% when the beams were strengthened with 2 meters (6.5 ft) of AA plates in AA90S2 specimens with an increase in the deflection up to 34.6%. The maximum strain measured by the strain gauges placed at two of the middle AA plates of AA90S2-1 reached around 0.0004, as shown in Fig. 7(b), which is less than 0.005, the average yield strain for the AA plate (5083-111). On the other hand, the load-deflection response for AA30 beams were unexpected since AA30S1 (21% increase in P_u, 60% in deflection) specimens achieved higher capacity than AA30S2 (8% increase) as shown in Fig. 8(a). The plates in AA30S2 did not provide the support expected to upgrade the capacity which was verified by the low strain measurements achieved and presented in Fig. 8(b). The angle and length of the plates in these specimens did not provide enough development bonded length around the crack to support, upgrade and reinforce the beam. Full depth long plates would provide the maximum bonded length and higher shear reinforcements for the deficient beams.

As stated earlier and presented in Fig. 9(a), AA45S specimens achieved the highest increase in the shear

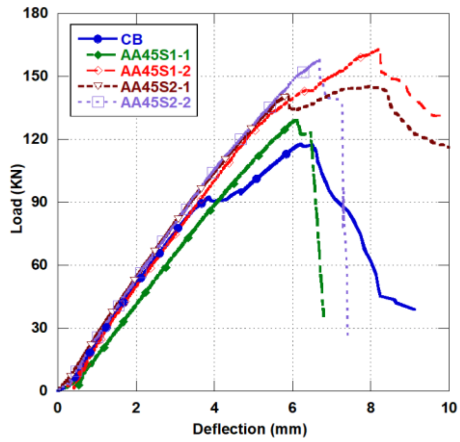

(a)

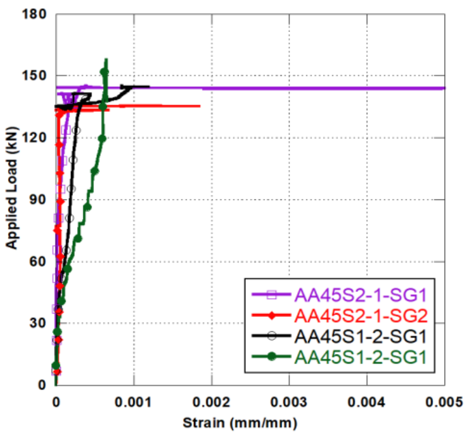

(b)

Fig. 9 Load deflection and strain results for AA45 beams (a) Load deflection response for AA45S1 and AA45S2 beams (b) AA plate Strain results for AA45S1 and AA45S2 specimen

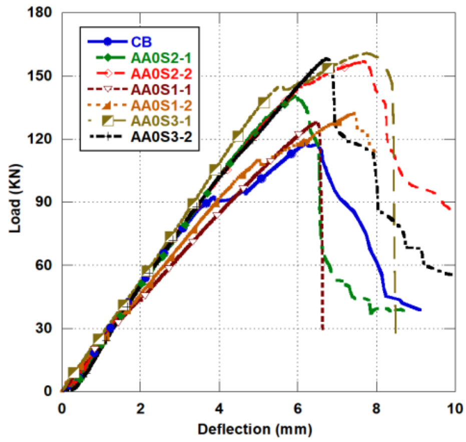

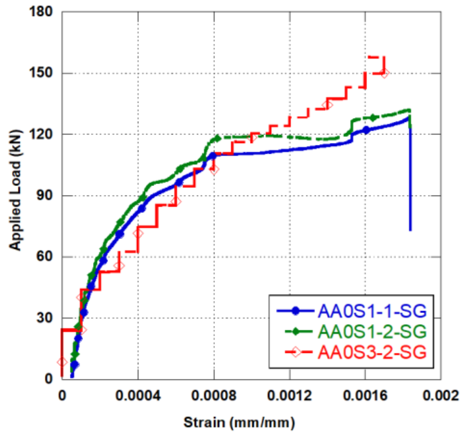

Fig. 10 Load deflection and strain results for AA0S beams (a) Load deflection response for AA0S beams (b) AA plate Strain results for AA0S

capacity (37%) and deflection (41.65%), compared to the control beam. The effectiveness of the 45° plates has been also confirmed with the high strain measurements that were observed on these plates at failure. Similarly to AA30 specimens, the reduction in the plates' spacing (increase in quantity) did not correlate consistently with the increase in the specimens shear capacity which is directly because of the lack of the full depth plates. For AA0S specimens, the load-deflection and load-plate strain response of the strengthened beams with different plates quantities are presented in Fig. 10. As shown, the AA0S beams that were strengthened with S1, S2 and S3 amount of plates failed at ultimate maximum loads of 132.2, 157, and 160.74 kN, respectively which correlates with an increase in the ultimate load by 12, 33, and 36%. Moreover, the deflection for AA0S1, AA0S2 and AA0S3 was increased by 28.6%, 32.7% and 33.6%, respectively. The AA0S ultimate load showed consistent results with the specimens shear capacity increase when S1 and S2 is compared. However, there was no significant change in the capacity between AA0S2 and AA0S3 specimens.

3.2 Failure modes

All AA strengthened beams failed by a diagonal tension failure crack as presented in Fig. 11. The cracking initiated with the appearance of flexural cracks. As the load increased, a single inclined crack appeared in the shear span, which progressed toward the load point and support region, leading to a diagonal tension failure.

Fig. 11 (b) and (c) presents AA45 specimens before and after failure. Fig. 11 (d) and (e) presents the shear crack progression for AA90 specimens. The crack progressed through the plates and caused partial-debonding for the plates located close to the crack for AA90S1 beams and full-debonding for the same plates in AA90S2 specimens. Similarly, AA30S1 failure crack path went through the plates without causing any partial or full-debonding and the load carrying capacity increased by 25%. However, AA30S2 specimen's crack progressed around the plates, as presented in Fig. 11 (f) and (g). This could have been avoided and the plates would have been more effective if they were provided in longer strips and were bonded at the full depth of the section for all AA strengthened specimens.

AA0S specimen's failure cracks are presented in Fig. 11 (h) through (j). These specimens had the shear crack progressed through the plates which caused partial and full-debonding for most of them. The diagonal shear crack was delayed and contained which resulted in 36% increase in the ultimate capacity. Although the failure patterns for

(a) Control beam

(b) AA45S1 Specimen before and after failure

(c) AA45S2 Specimen before and after failure

(d) AA90S1 Specimen before and after failure

(e) AA90S2 Specimen before and after failure

(f) AA30S1 Specimen before and after failure

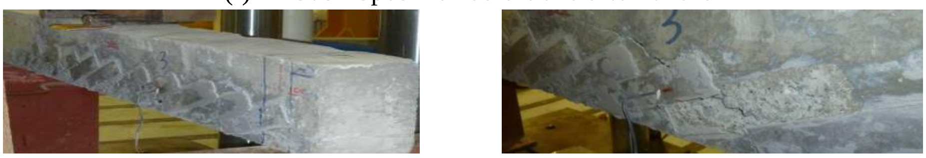

(g) AA30S2 Specimen before and after failure

(h) AA0S1 Specimen before and after failure

(i) AA0S2 Specimen before and after failure

(j) AA0S3 Specimen before and after failure

Fig. 3 Failure modes for AA strengthened beams

AA0S1, S2 and S3 were consistent, the improvements in the ultimate capacity were as consistent. When two meters of plates were used instead of one, the percentage upgrade in the capacity increased from 12 to 34%. However, when three meters were utilized, there was no significant change in the ultimate load compared to the specimens with two meters. Similarly to the AA0S results, using one meter of 45^o plates in AA45S1 beams was effective enough to increase the capacity up to 37%, which was not significantly differently from specimens with two meters of bonded AA plates.

4. Shear strength predictions for AA strengthened beams

In recent years, many studies investigated shear deficient RC beams strengthened with FRP experimentally and analytically and many of these investigations have led to several design models models (Carolin and Täljsten 2005, Islam *et al*. 2005, Khalifa *et al*. 1998, Carolin and Täljsten 2005, Chaallal *et al*. 1998, Chajes *et al*. 1995, Chen and Teng 2003, Triantafillou and Antonopoulos 2000, Chen *et al*. 2017). Some of the proposed models have been adopted in design guidelines like ACI-440.2R (2008), TR55 (2000) and FIB (2001). Most of these design models assumes that the shear capacity of the FRP shear-strengthened beams (V_u) is a summation of the concrete shear contributions (V_c), stirrups contributions (V_s) and the externally bonded FRP sheets or plates contributions (V_f), based on simple superposition (i.e., $V_u=V_c+V_s+V_f$).

Using the equations adopted by the American concrete institute committee ACI 440 the international federation for structural concrete and the concrete society in the UK codes developed for FRP external reinforcement, the shear capacity of AA shear-strengthened beams will be calculated and compared to the experimental results. These equations will be used as a benchmark to evaluate the capacity of such beams and modifications will be recommended for better results.

4.1 American concrete institute committee, ACI 440.2R

ACI 440.2R-08 is the American guide for the design and construction of externally bonded FRP systems for strengthening concrete structures. The following Eqs. (1)-(10), which is developed for RC beams strengthened with FRP, has been used to predict the shear strength of the AA strengthened RC beams. These equations are derived based on an assumed crack pattern (Khalifa *et al*. 1998). In the calculations, safety factors will be assumed to be 1.0 in the design equations to predict the nominal shear capacity of strengthened specimens.

$$V_n = V_c + V_s + \Psi V_f \tag{1}$$

where

$$\mathrm{V_c} = 0.17\sqrt{f_c'}\,\mathrm{b_w\,d} \tag{2}$$

$$V_f = \frac{A_{fv} f_{fe}(\sin\alpha + \cos\alpha) d_{fv}}{S_f} \tag{3}$$

$$A_{fv} = 2nt_f w_f \tag{4}$$

$$f_{fe} = \varepsilon_{fe} E_f \tag{5}$$

$$\varepsilon_{fe} = k_v \varepsilon_{fu} \tag{6}$$

$$k_v = \frac{k_1 k_2 L_e}{11900\ \varepsilon_{fu}} \tag{7}$$

$$k_2 = \frac{d_{fv} - 2L_e}{d_{fv}} \tag{8}$$

$$L_e = \frac{23300}{(nt_f E_f)^{0.58}} \tag{9}$$

$$k_1 = \left(\frac{f_c'}{27.6}\right)^{\frac{2}{3}} \tag{10}$$

4.2 International federations of structural concrete

According to FIB14, the following design Eqs. (11)-(14) are recommended to calculate the FRP contribution to the shear capacity of RC beams. These equations are based on the model of Triantafillou and Antonopoulos (2000).

$$V_{Rd} = V_{cd} + V_{wd} + V_{fd} \tag{11}$$

where

$$V_{fd} = 0.9\varepsilon_{fd,e} E_{fu} \rho_f b_w d(\cot\theta + \cot\alpha)\sin\alpha \tag{12}$$

$$\rho_f = \left(\frac{2t_f}{b_w}\right)\left(\frac{b_f}{s_f}\right) \tag{13}$$

$$\varepsilon_{fe} = \min\left\{\left(0.65\left(\frac{(f_{cm})^{2/3}}{E_{fu}\rho_f}\right)^{0.56}\right)\times 10^{-3}\ or\ \ 0.17\left(\frac{(f_{cm})^{2/3}}{E_{fu}\rho_f}\right)^{0.3}\varepsilon_{fu}\right\} \tag{14}$$

4.3 The concrete society in the UK

TR55 is the design guidance for strengthening concrete structures using fiber composite materials in UK. The following Eqs. (15)-(23) is used to predict the shear strength of RC beams externally strengthened with FRP sheets and plates according to the TR55 design guidelines. The model has been developed in accordance with Eurocode (BS EN 1992-1-1) terms and concept, and states that the shear capacity of any concrete beam strengthened in shear with FRPs shall be determined as follows

$$V_{\mathrm{Re}} = V_{Rc} + V_{RI} + V_{Rf} \tag{15}$$

where

Table 4 Measured and predicted ultimate loads for all specimens

		ACI 440			FIB 14			TR55		
Specimen*	Measured (Exp.) (kN)	*Pred*. (ψ_f=1) (kN)	P_{exp}/P_{pre}	MAPE (%)	*Pred*.(No *k*) (kN)	P_{exp}/P_{pre}	MAPE (%)	*Pred* (3.5) (kN)	P_{exp}/P_{pre}	MAPE (%)
AA90S1 - 1	139.53	117.97	1.18	15.45	126.00	1.11	9.70	94.58	1.48	32.21
AA90S1 - 2	119.40	117.97	1.01	1.20	126.00	0.95	5.52	94.58	1.26	20.79
AA90S2 - 1	126.48	163.49	0.77	29.26	156.20	0.81	23.50	217.65	0.58	72.08
AA90S2 - 2	147.63	163.49	0.90	10.74	156.20	0.95	5.81	217.65	0.68	47.43
AA30S1 - 1	143.48	118.09	1.22	17.70	132.74	1.08	7.48	110.89	1.29	22.72
AA30S1 - 2	136.63	118.09	1.16	13.57	132.74	1.03	2.85	110.89	1.23	18.84
AA30S2 - 1	126.48	183.95	0.69	45.44	179.33	0.71	41.78	208.47	0.61	64.83
AA30S2 - 2	123.08	183.95	0.67	49.46	179.33	0.69	45.70	208.47	0.59	69.38
AA45S1 - 1	129.45	120.41	1.08	6.98	135.37	0.96	4.58	112.75	1.15	12.90
AA45S1 - 2	162.79	120.41	1.35	26.03	135.37	1.20	16.84	112.75	1.44	30.74
AA45S2 - 1	145.17	188.60	0.77	29.92	183.60	0.79	26.47	213.78	0.68	47.26
AA45S2 - 2	157.83	188.60	0.84	19.50	183.60	0.86	16.33	213.78	0.74	35.45
Average			0.97	22.10		0.93	17.21		0.97	39.55

* duplicate experimental specimens are designated as Exp-1 and Exp-2 in Fig.12

$$V_{Rf} = \left(\frac{1}{\gamma_{mF}}\right) A_{fs}\left(E_{fd}\,\varepsilon_{fe}\right)\sin\beta(1+\cot\beta)\left(\frac{d_f}{S_f}\right) \tag{16}$$

$$\rho_f = \left(\frac{2t_f}{b_w}\right)\left(\frac{b_f}{s_f}\right) \tag{17}$$

$$L_e = \frac{461.3}{\left(t_f E_{fd}\right)^{0.58}} \tag{18}$$

$$w_{fe} = d_f - 2L_e \tag{19}$$

$$A_{fs} = 2t_f w_{fe} \tag{20}$$

$$\varepsilon_{fu} = \frac{\varepsilon_{fk}}{\gamma_{mf}} \tag{21}$$

$$\varepsilon_{fe} = \varepsilon_{fu}\left[0.5622\left(\rho_f E_{fd}\right)^2 - 1.2188\,\rho_f E_{fd} + 0.778\right] \tag{22}$$

$$V_{Rf} = \left(\frac{1}{\gamma_{mF}}\right) A_{fs}\left(E_{fd}\,\varepsilon_{fe}\right)\sin\beta(1+\cot\beta)\left(\frac{d_f}{S_f}\right) \tag{23}$$

4.4 Summary of the predicted results

Table 4 and Fig. 12 present the results of the statistical measurements of the predictions of the ACI, TR55, and FIB14 codes. As stated earlier, these three design models assume that the shear capacity of the shear-strengthened beams (V_u) is a summation of the concrete shear contributions (V_c), stirrups contributions (V_s) and the externally bonded FRP contributions (V_f) based on simple superposition (i.e., V_u=V_c+V_s+V_f). However, the three components (V_c+V_s+V_f) might not achieve their ultimate values simultaneously and an interaction may exist among them during the failure process which will results in a shear strength less than the summation of the three components (Khalifa *et al*. 1998, Chaallal *et al*. 1998).

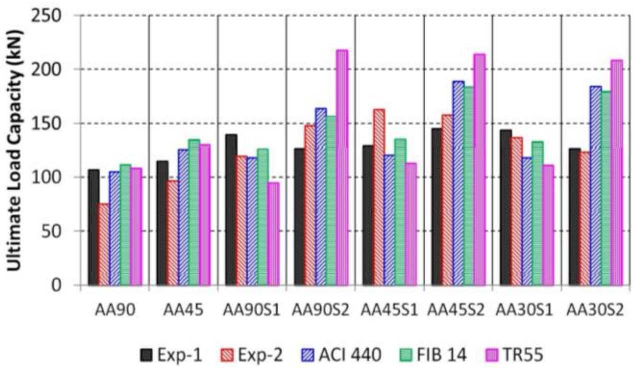

Fig. 12 Measured and predicted ultimate loads

As observed in Table 4, the Mean Absolute Percent Error (MAPE) of the prediction by each of the four codes is relatively comparable with maximum MAPE of 69.38% depicted by TR55 prediction for specimen AA30S2-2. The average of MAPE for all code predictions ranges between 17.21% and 39.55%. The results clearly shows that ACI440 and FIB14 predictions have comparable accuracy, with the FIB14 appear to be the most accurate and TR55 is the least accurate in predicting the shear strength of the tested beams. The normalized mean square error (NMSE) for ACI440, FIB14 and TR55 are 7.07, 4.87 and 20.17, respectively which further confirms the accuracy of FIB14 predictions. The recommended additional reduction factor (Ψ_f) in the ACI equation was assumed to be 1.0 since the values suggested in the code are based on a reliability analysis of FRP data. Similarly in TR55 predictions, the partial safety factor (γ_f=γ_{th}) was not applied since the suggested values are based on the FRP laminates mechanical of properties and method of manufacturing. For the FIB14 predictions, a material safety factor of 1.5 was applied for the concrete, since the bond failure occurred in the concrete.

Further investigation is required for the AA plate's contribution in the shear capacity of the RC beams. There are many shortcomings in the models presented in the current codes for FRP that contributed in the high percentage difference between the code and the experimental values for the AA strengthened beams. For example, ACI 440.2R-08 equations fails to accurately predict the shear capacity of the FRP strengthened beams when the thickness of the FRP laminates is high, which includes the AA plate's thickness presented in the current study. The design guidelines are based on Triantafillou's statement that contribution to shear strength will increase with low values of axial stiffness (ASTMB557M). In addition, The ACI method for the analysis of shear and diagonal tension in beams is empirical and lacks the proper model for the behavior of beams subjected to shear combined with bending (Chen *et al*. 2017, Dhahir 2018).

5. Conclusions

The paper focused on the investigating of the AA plates in strengthening reinforced concrete (RC) beams in shear. The AA plates were bonded to eighteen RC beam specimens via epoxy adhesives with different orientations and spacing. The following conclusions can be drawn from the analysis of experimental and analytical results:

• Aluminum alloy plates can be used to externally strengthen reinforced concrete beams in shear. Based on the results of this investigation, the increase in shear capacity reached up to 37%. Therefore, using aluminum alloy plates is a highly effective technique in increasing the beam shear capacity.

• The spacing and orientation of AA plates, as external strengthening material, has a major effect on the load-carrying capacity of the strengthened RC beams. As observed, the 45° AA plate orientation contributed in upgrading the ultimate load and deflection of the concrete beams.

• The full potential of the AA plates in strengthening RC beams should be further investigated using full depth plates. This will assure maximum bond length around the cracks and delay its propagation which expected to result in higher beam's capacity, deflection and ductility.

• The design codes developed for FRP (ACI440, FIB14 and TR55) composites can predict, to some degree of accuracy, the shear capacity of RC beams strengthened with externally bonded AA plates. However, more specialized models need to be developed for AA strengthened beams that take into consideration the properties of the AA plates applied. This requires further data and experimental studies that to investigate the effect of several variables on the shear strength of reinforced concrete beams externally strengthened with AA plates.

• The results of this investigation validates the viability of using AA plates as an alternative to the prevailing FRP laminates and steel plates as an externally bonded shear strengthening material.

• The effect of the AA plates' length and thickness in improving the beams capacity and ductility should be further investigated to find the optimum plates dimensions for the most effective strengthening system.

Acknowledgment

The research described in this paper was financially supported by the American University of Sharjah. Their support is highly appreciated.

References

AALCO METALS LIMITED (Accessed 15 January 2017) http://www.aalco.co.uk/products/aluminium.aspx

Abdalla, J.A., Abu-Obeidah, A. and Hawileh, R.A. (2011), "Behaviour of shear deficient reinforced concrete beams with externally bonded aluminum alloy plates", *The 2011 World Congress on Advances in Structural Engineering and Mechanics*, September.

Abdalla, J.A., Abu-Obeidah, A.S., Hawileh, R.A. and Rasheed, H.A. (2016), "Shear strengthening of reinforced concrete beams using externally-bonded aluminum alloy plates: An experimental study", *Constr. Build. Mater.*, **128**, 24-37. https://doi.org/10.1016/j.conbuildmat.2016.10.071.

Abdalla, J.A., Hraib, F.H., Hawileh, R.A. and Mirghani, A.M. (2017), "Experimental investigation of bond-slip behavior of aluminum plates adhesively bonded to concrete", *J. Adhes. Sci. Technol.*, **31**(1), 82-99. https://doi.org/10.1080/01694243.2016.1204741.

Abdel-Kareem, A.H. (2014), "Shear strengthening of reinforced concrete beams with rectangular web openings by FRP composites", *Adv. Concrete Constr.*, **2**(4), 281-300. https://doi.org/10.12989/acc.2014.2.4.281.

Abu-Obeidah, A., Hawileh, R. and Abdalla, J.A. (2012), "Finite element modeling of shear deficient beams bonded with aluminum plates", *Proceedings of the Eleventh International Conference on Computational Structures Technology*, Dubrovnik, Croatia.

Abu-Obeidah, A., Hawileh, R.A. and Abdalla, J.A. (2015), "Finite element analysis of strengthened RC beams in shear with aluminum plates", *Comput. Struct.*, **147**, 36-46. https://doi.org/10.1016/j.compstruc.2014.10.009.

Abu-Obeidah, A.S. (2012), "Behaviour of shear deficient reinforced concrete beams with externally bonded aluminum plates", Master Thesis, American University of Sharjah, Sharjah, UAE.

Adhikary, B.B. and Mutsuyoshi, H. (2006), "Shear strengthening of RC beams with web-bonded continuous steel plates", *Constr. Build. Mater.*, **20**(5), 296-307. https://doi.org/10.1016/j.conbuildmat.2005.01.026.

Ahmad, H., Hameed, R., Riaz, M.R. and Gillani, A.A. (2018), "Strengthening of concrete damaged by mechanical loading and elevated temperature", *Adv. Concrete Constr.*, **6**(6), 645-658. : https://doi.org/10.12989/acc.2018.6.6.645.

Akroush, N., Almahallawi, T., Seif, M. and Sayed-Ahmed, E.Y. (2017), "CFRP shear strengthening of reinforced concrete beams in zones of combined shear and normal stresses", *Compos. Struct.*, **162**, 47-53. https://doi.org/10.1016/j.compstruct.2016.11.075.

Al-Sulaimani, G.J., Sharif, A., Basunbul, I.A., Baluch, M.H. and Ghaleb, B.N. (1994), "Shear repair for reinforced concrete by fiberglass plate bonding", *Struct. J.*, **91**(4), 458-464.

Ali, A., Abdalla, J., Hawileh, R. and Galal, K. (2014), "CFRP mechanical anchorage for externally strengthened RC beams under flexure", *Phys. Procedia*, **55**, 10-16.

https://doi.org/10.1016/j.phpro.2014.07.002.

Ali, N., Mohamad, N., Jayaprakash, J., Tee, K.F. and Mendis, P. (2016), "Shear strengthening and shear repair of 2-Span continuous RC beams with CFRP strips", *J. Compos. Constr.*, **21**(3), 04016099. https://doi.org/10.1061/(ASCE)CC.1943-5614.0000756.

American Concrete Institute. Committee 440 (2002), Guide for the Design and Construction of Externally Bonded FRP Systems for Strengthening Concrete Structures: ACI 440.2 R-02, American Concrete Institute.

ASTM International. Committee B07 on Light Metals and Alloys (2015), Standard Test Methods for Tension Testing Wrought and Cast Aluminum-and Magnesium-alloy Products (metric), ASTM International.

Aykac, S., Kalkan, I., Aykac, B., Karahan, S. and Kayar, S. (2012), "Strengthening and repair of reinforced concrete beams using external steel plates", *J. Struct. Eng.*, **139**(6), 929-939. https://doi.org/10.1061/(ASCE)ST.1943-541X.0000714.

Azam, R. and Soudki, K. (2014), "FRCM strengthening of shear-critical RC beams", *J. Compos. Constr.*, **18**(5), 04014012. https://doi.org/10.1061/(ASCE)CC.1943-5614.0000464.

Baghi, H. and Barros, J.A. (2016), "Shear strengthening of reinforced concrete T-beams with hybridcomposite plate", *J. Compos. Constr.*, **20**(6), 04016036. https://doi.org/10.1061/(ASCE)CC.1943-5614.0000693.

Carolin, A. and Täljsten, B. (2005), "Experimental study of strengthening for increased shear bearing capacity", *J. Compos. Constr.*, **9**(6), 488-496. https://doi.org/10.1061/(ASCE)1090-0268(2005)9:6(488).

Carolin, A. and Täljsten, B. (2005), "Theoretical study of strengthening for increased shear bearing capacity", *J. Compos. Constr.*, **9**(6), 497-506. https://doi.org/10.1061/(ASCE)1090-0268(2005)9:6(497).

Chaallal, O., Nollet, M.J. and Perraton, D. (1998), "Shear strengthening of RC beams by externally bonded side CFRP strips", *J. Compos. Constr.*, **2**(2), 111-113. https://doi.org/10.1061/(ASCE)1090-0268(1998)2:2(111).

Chajes, M.J., Januszka, T.F., Mertz, D.R., Thomson, T.A. and Finch, W.W. (1995), "Shear strengthening of reinforced concrete beams using externally applied composite fabrics", *Struct. J.*, **92**(3), 295-303.

Chajes, M.J., Januszka, T.F., Mertz, D.R., Thomson, T.A. and Finch, W.W. (1995), "Shear strengthening of reinforced concrete beams using externally applied composite fabrics", *Struct. J.*, **92**(3), 295-303.

Chakrabortty, A. and Khennane, A. (2014), "Failure mechanisms of hybrid FRP-concrete beams with external filament-wound wrapping", *Adv. Concrete Constr.*, **2**(1), 57-75. http://dx.doi.org/10.12989/acc.2014.2.1.057.

Chen, G.M., Li, S.W., Fernando, D., Liu, P.C. and Chen, J.F. (2017), "Full-range FRP failure behaviour in RC beams shear-strengthened with FRP wraps", *Int. J. Solid. Struct.*, **125**, 1-21. https://doi.org/10.1016/j.ijsolstr.2017.07.019.

Chen, J.F. and Teng, J.G. (2003), "Shear capacity of fiber-reinforced polymer-strengthened reinforced concrete beams: Fiber reinforced polymer rupture", *J. Struct. Eng.*, **129**(5), 615-625. https://doi.org/10.1061/(ASCE)0733-9445(2003)129:5(615).

Comité Européen de Normalisation (2004), Design of Concrete Structures-Part 1-1: General Rules and Rules for Buildings, Eurocode 2, EN 1992-1-1: 2004: E.

Dhahir, M.K. (2018), "Strut and tie modeling of deep beams shear strengthened with FRP laminates", *Compos. Struct.*, **193**, 247-259. https://doi.org/10.1016/j.compstruct.2018.03.073.

Du Béton, F.I. (2001), "Externally bonded FRP reinforcement for RC structures", *Bulletin*, **14**, 138.

Dursun, T. and Soutis, C. (2014), "Recent developments in advanced aircraft aluminium alloys", *Mater. Des.*, **56**, 862-871. https://doi.org/10.1016/j.matdes.2013.12.002.

Editor Report (1965), "The aluminum and concrete controversy. Publication #C650369", Concrete Construction Magazine, The Aberdeen Group.

Esfandiari, S. and Esfandiari, J. (2016), "Simulation of the behaviour of RC columns strengthen with CFRP under rapid loading", *Adv. Concrete Constr.*, **4**(4), 319-332. https://doi.org/10.12989/acc.2016.4.4.319.

Foster, R.M., Brindley, M., Lees, J.M., Ibell, T.J., Morley, C.T., Darby, A.P. and Evernden, M.C. (2016), "Experimental investigation of reinforced concrete T-beams strengthened in shear with externally bonded CFRP sheets", *J. Compos. Constr.*, **21**(2), 04016086. https://doi.org/10.1061/(ASCE)CC.1943-5614.0000743.

Hawileh, R., Abdalla, J., Nawaz, W., Alzeer, A., Muwafi, R. and Faridi, A. (2014), "Strengthening reinforced concrete beams in flexure using hardwire steel fiber sheets", *Proceedings of CICE,* Vancouver, Canada, August.

Hawileh, R.A., Nawaz, W. and Abdalla, J.A. (2018), "Flexural behavior of reinforced concrete beams externally strengthened with Hardwire Steel-Fiber sheets", *Constr. Build. Mater.*, **172**, 562-573. https://doi.org/10.1016/j.conbuildmat.2018.03.225.

Hawileh, R.A., Nawaz, W., Abdalla, J.A. and Saqan, E.I. (2015), "Effect of flexural CFRP sheets on shear resistance of reinforced concrete beams", *Compos. Struct.*, **122**, 468-476. https://doi.org/10.1016/j.compstruct.2014.12.010.

Hawileh, R.A., Rasheed, H.A., Abdalla, J.A. and Al-Tamimi, A.K. (2014), "Behavior of reinforced concrete beams strengthened with externally bonded hybrid fiber reinforced polymer systems", *Mater. Des.*, **53**, 972-982. https://doi.org/10.1016/j.matdes.2013.07.087.

Hosseinpour, F. and Abbasnia, R. (2014), "Experimental investigation of the stress-strain behavior of FRP confined concrete prisms", *Adv. Concrete Constr.*, **2**(3), 177-192. http://dx.doi.org/10.12989/acc.2014.2.3.177.

Hosseinpour, F. and Abdelnabya A.E. (2015), "Statistical evaluation of the monotonic models for FRP confined concrete prisms", *Adv. Concrete Constr.*, **3**(3), 161-185. https://doi.org/10.12989/acc.2015.3.3.161.

Islam, M.R., Mansur, M.A. and Maalej, M. (2005), "Shear strengthening of RC deep beams using externally bonded FRP systems", *Cement Concrete Compos.*, **27**(3), 413-420. https://doi.org/10.1016/j.cemconcomp.2004.04.002.

Jana, D. and Tepke, D.G. (2010), "Corrosion of aluminum metal in concrete-a case study", *The 32nd International Conference on Cement Microscopy, ICMA*, March.

Jumaat, M.Z., Rahman, M.A., Alam, M.A. and Rahman, M.M. (2011), "Premature failures in plate bonded strengthened RC beams with an emphasis on premature shear: A review", *Int. J. Phys. Sci.*, **6**(2), 156-168. https://doi.org/10.5897/IJPS10.369.

Khalifa, A. and Nanni, A. (2000), "Improving shear capacity of existing RC T-section beams using CFRP composites", *Cement Concrete Compos.*, **22**(3), 165-174. https://doi.org/10.1016/S0958-9465(99)00051-7.

Khalifa, A., Gold, W.J., Nanni, A. and MI, A.A. (1998), "Contribution of externally bonded FRP to shear capacity of RC flexural members", *J. Compos. Constr.*, **2**(4), 195-202. https://doi.org/10.1061/(ASCE)1090-0268(1998)2:4(195).

Kissell, J.R. and Ferry, R.L. (2002), *A Guide to Their Specifications and Design*, John Wiley & Sons, INC.

Linberg, R.I. (1960), *Aluminum in Concrete*, Publication #C600008, Concrete Construction Magazine, The Aberdeen Group.

McGeary, F.L. (1966), "Performance of aluminium in concrete containing chlorides", *J. Proc.*, **63**(2), 247-266.

Mesbah, H.A. and Benzaid, R. (2017), "Damage-based stress-

strain model of RC cylinders wrapped with CFRP composites", *Adv. Concrete Constr.*, **5**(5), 539-561. https://doi.org/10.12989/acc.2017.5.5.539.
Metwally, I.M. (2014), "Three-dimensional finite element analysis of reinforced concrete slabs strengthened with epoxy-bonded steel plates", *Adv. Concrete Constr.*, **2**(2), 91-108. http://dx.doi.org/10.12989/acc.2014.2.2.091.
Mirghani, A.M., Abdalla, J.A. and Hawileh, R.A. (2017), "Modeling and simulation of bond-slip behavior of Aluminum Alloy plates adhesively bonded to concrete", *Modeling, Simulation, and Applied Optimization (ICMSAO), 2017 7th International Conference on*, 1-5.
Rasheed, H.A., Abdalla, J., Hawileh, R. and Al-Tamimi, A.K. (2017), "Flexural behavior of reinforced concrete beams strengthened with externally bonded Aluminum Alloy plates", *Eng. Struct.*, **147**, 473-485. https://doi.org/10.1016/j.engstruct.2017.05.067.
Razavi, S.V., Jumaat, M.Z., EI-Shafie, A.H. and Ronagh, H.R. (2015), "Load-deflection analysis prediction of CFRP strengthened RC slab using RNN", *Adv. Concrete Constr.*, **3**(2), 91-102. https://doi.org/10.12989/acc.2015.3.2.091.
Sikadur-30® , https://www.sika-distributor.com/pdf/sikadur30/pds-cpd-Sikadur30-us.pdf
Sumathi, A. and Arun Vignesh, S. (2017), "Study on behavior of RCC beams with externally bonded FRP members in flexure", *Adv. Concrete Constr.*, **5**(6), 625-638. https://doi.org/10.12989/acc.2017.5.6.625.
Szumigała, M. and Polus, Ł. (2015), "Applications of aluminium and concrete composite structures", *Procedia Eng.*, **108**, 544-549. https://doi.org/10.1016/j.proeng.2015.06.176.
Täljsten, B. and Elfgren, L. (2000), "Strengthening concrete beams for shear using CFRP-materials: evaluation of different application methods", *Compos. Part B: Eng.*, **31**(2), 87-96. https://doi.org/10.1016/S1359-8368(99)00077-3.
The Concrete Society (2000), "Design guidance for strengthening concrete structures using fibre composites materials", Technical Report no. 55, 2nd Edition, Report of a Concrete Society Committee, Berkshire, UK.
Triantafillou, T.C. (1998), "Shear strengthening of reinforced concrete beams using epoxy-bonded FRP composites", *ACI Struct. J.*, **95**, 107-115.
Triantafillou, T.C. and Antonopoulos, C.P. (2000), "Design of concrete flexural members strengthened in shear with FRP", *J. Compos. Constr.*, **4**(4), 198-205. https://doi.org/10.1061/(ASCE)1090-0268(2000)4:4(198).
Wang, L. and Su, R.K.L. (2013), "A unified design procedure for preloaded rectangular RC columns strengthened with post-compressed plates", *Adv. Concrete Constr.*, **5**(5), 539-561. http://dx.doi.org/10.12989/acc.2013.1.2.163.
Wu, G., Zeng, Y.H., Wu, Z.S. and Feng, W.Q. (2012), "Experimental study on the flexural behavior of RC beams strengthened with steel-wire continuous basalt fiber composite plates", *J. Compos. Constr.*, **17**(2), 208-216. https://doi.org/10.1061/(ASCE)CC.1943-5614.0000328.
Xing, G. and Ozbulut, O.E. (2016), "Flexural performance of concrete beams reinforced with aluminum alloy bars", *Eng. Struct.*, **126**, 53-65. https://doi.org/10.1016/j.engstruct.2016.07.032.
Zhang, Z. and Hsu, C.T.T. (2005), "Shear strengthening of reinforced concrete beams using carbon-fiber-reinforced polymer laminates", *J. Compos. Constr.*, **9**(2), 158-169. https://doi.org/10.1061/(ASCE)1090-0268(2005)9:2(158).

CC

Notations

A_{fv}	area of FRP shear reinforcement with spacing s, (mm^2)
A_{fs}	area of FRP shear reinforcement
b_w	minimum width of cross section over the effective depth
b_w	web width or diameter of circular section, (mm) – FIB14
b_f	width of the strips of the bonded reinforcment (mm)
d	effective depth of cross section (mm)
d_{fv}	effective depth of the FRP shear reinforcement, (mm)
ε_{fe}	*effective strain level in FRP reinforcement attained at failure, (mm/mm)
E_{fd}	design Elastic modulus of FRP (GPa)
E_{fu}	elastic modulus of FRP in the principle fiber orientation
E_f	tensile modulus of elasticity of FRP plates, (MPa)
f_{cu}	cube strength of concrete (MPa)
f_{fe}	effective stress in the FRP; stress level attained at section failure, (MPa)
k	reduction factor (k=0.8)
L_e	active bond length of FRP laminates, (mm)
n	number of plies of FRP reinforcement
s_f	spacing between the strips of the bodned reiforcment (mm)
t_f	nominal thickness of one ply of FRP reinforcment, (mm)
t_f	thickness of bonded reinforcement (mm)
V_{Rc}	concrete contribution to shear capacity
V_{cd}	concrete contribution to shear capacity
V_{Tf}	FRP contribution to shear capacity
V_{fd}	FRP contribution to shear capacity
V_c	nominal shear strength provided by concrete (N)
V_f	nominal shear strength provided by FRP plates (N)
V_s	nominal shear strength provided by shear reinforcement (N)
w_{fe}	effective width of the FRP
w_f	width of FRP reinforcing plies, (mm)
w_f	width of the strips of the bonded reinforcment (mm)
$\gamma_w=\gamma_{fb}$	partial safety factor (if failure involves fracture)
γ_{mF}	partail saftey factor for FRP
Ψi	additional FRP strength-reduction factor
ε_{fu}	ultimate rupture strain of FRP reinforcement, (mm/mm)
ε_{fu}	design ultimate failure strain in FRP
$\varepsilon_{fu,e}$	design value of the effective FRP strain
ρ_f	FRP reinforcement ratio equal to $\frac{2t_f \sin\alpha}{b_w}$ for continuously bonded shear reinforcement or $\left(\frac{2t_f}{b_w}\right)\left(\frac{b_f}{s_f}\right)$ for FRP reinforcement in the form of strips
ρ_f	FRP reinforcement ratio equal to $\frac{2t_f \sin\alpha}{b_w}$ for continuously bonded shear reinforcement or

$\left(\frac{2t_f}{b_w}\right)\left(\frac{b_f}{s_f}\right)$ for FRP reinforcement in the form of strips

β angle between principal fibre orientation and longitudinal axis of member

α angle between principal fibre orientation and longitudinal axis of member

θ angle of diagonal crack with respect to the member axis, assumed equal to 45^o